ORIGINAL ARTICLE

A Study on Ikaite Growth in the Presence of Phosphate

Samuel B. Strohm[1] · Giuseppe D. Saldi[2,3] · Vasileios Mavromatis[2,4] ·
Wolfgang W. Schmahl[1] · Guntram Jordan[1]

Abstract

Phosphate is a common component in natural growth solutions of ikaite. Although phosphate often occurs as a minor constituent, its presence may promote the formation of ikaite as it significantly inhibits the precipitation of calcite. The interactions of phosphate with ikaite and the role of a potential uptake of phosphate by ikaite, however, are poorly understood. In this study, the influence of phosphate on ikaite growth at 1 °C was investigated. Ikaite- and calcite-seeded growth experiments were conducted in cryo-mixed-flow reactors at saturation ratios $1.5 \leq \Omega_{ikaite} \leq 2.9$ (Ω = ionic activity product/solubility product). From these growth experiments, the rate constant $k = 0.10 \pm 0.03$ μmol/m^2/s and the reaction order $n = 0.8 \pm 0.3$ were derived for ikaite. The reaction order implies a transport- or adsorption-controlled growth mechanism which supports a low energy pathway of ikaite growth via an attachment of hydrous $CaCO_3^0$ complexes without any extensive dehydration of aqueous species as, for instance, required for calcite growth. A potential depletion of aqueous phosphate due to an uptake by ikaite growth was not detectable. Furthermore, growth retardation by phosphate, as known for calcite growth, was not evident. Thus, a significant incorporation of phosphate into growing ikaite could be precluded for the conditions applied in this study. The observed lack of incorporation of phosphate agrees with the previously suggested growth mechanism via the attachment of hydrous $CaCO_3^0$ complexes which likely does not facilitate substantial substitution of carbonate by phosphate ions.

Keywords Ikaite growth kinetics · Hydrous calcium carbonate minerals · Phosphate growth inhibition · Trace element incorporation

✉ Guntram Jordan
  jordan@lmu.de

1   Department für Geo- und Umweltwissenschaften (Sektion Kristallographie), Ludwig-Maximilians-Universität München, Theresienstraße 41, 80333 Munich, Germany

2   Géosciences Environnement Toulouse (GET), CNRS-UPS-OMP UMR5563, 14 Avenue Edouard Belin, 31400 Toulouse, France

3   Dipartimento di Fisica e Geologia, Università di Perugia, Via Pascoli 35, 06123 Perugia, Italy

4   Institut für Geologie, Universität Bern, Baltzerstraße 1+3, 3012 Bern, Switzerland

1 Introduction

Ikaite (CaCO$_3$×6H$_2$O) is a calcium carbonate mineral which typically occurs in cold regions of the Earth ($T < 7$ °C; e.g. Bischoff et al. 1993a; Ito 1996; Stockmann et al. 2022). Among the known occurrences, the widespread appearance of ikaite in sea ice (Dieckmann et al. 2008, 2010) received particular interest as it may provide an abiotic pathway of carbon transport between the atmosphere and surface oceanic water (e.g. Delille et al. 2014; Geilfus et al. 2013, 2016). The precipitation and dissolution of ikaite concomitant with the formation and melting of sea ice could be an effective carbon pump (Delille et al. 2014; Rysgaard et al. 2007) and, thus, might have important implications for the polar carbon cycle.

The formation conditions of ikaite, however, are complex. Due to its metastability under Earth surface conditions (Marland 1975), the appearance of ikaite requires particular physicochemical parameters favouring its precipitation over the formation of the more stable anhydrous calcium carbonate minerals (calcite, aragonite, and vaterite). Previous studies showed that low temperatures (Johnston et al. 1916; Stockmann et al. 2018; Tollefsen et al. 2020; Zhou et al. 2015), alkaline solution conditions (Boch et al. 2015; Hu et al. 2015) or the presence of foreign mineral surfaces (Strohm et al. 2022) can promote ikaite nucleation. Furthermore, ikaite persistence requires a continuous inhibition of its impending transformation into anhydrous CaCO$_3$-minerals. In this regard, both aqueous Mg^{2+} and phosphate ions may promote the formation and persistence of ikaite (Bischoff et al. 1993a; Buchardt et al. 2001; Hu et al. 2014; Stockmann et al. 2018; Tollefsen et al. 2018).

In sea water, phosphate is a minor component with a concentration range of 0–3.2 μM (Millero 2013). A retardation of calcite and aragonite crystallization was verified at aqueous phosphate concentrations down to 1 μM and 0.25 μM for calcite (Lin and Singer 2006) and aragonite (Tadier et al. 2017), respectively. Dissolved phosphate, thus, may support the formation of ikaite in sea water to some degree and may even become a crucial parameter at elevated concentrations ($\sim$ 400 μM) (Zhou et al. 2015). Irrespective of the actual phosphate concentration, it remained ambiguous, whether the presence of phosphate in sea water is mandatory for the nucleation of ikaite in all settings (Hu et al 2014, 2015; Stockmann et al. 2018; Tollefsen et al. 2020; Zhou et al. 2015).

In aqueous solutions, in general, a depletion of phosphate concentrations can be caused by nucleation of calcium phosphate minerals (e.g. Stumm and Leckie 1970) and, as revealed in laboratory studies for calcite, by adsorption of phosphate ions on crystal surfaces (e.g. Sø et al. 2011; Suzuki et al. 1986; van der Weijden et al. 1997) or an uptake by amorphous phases (e.g. Habraken et al. 2015; Kababya et al. 2015; Zou et al. 2020, 2021). Furthermore, phosphate coprecipitation was observed when calcite growth inhibition was incomplete (e.g. House and Donaldson 1986; Ishikawa and Ichikuni 1981; Kitano et al. 1978).

Apart from the effects of phosphate on calcite, potential interactions between phosphate and ikaite need to be considered for a better understanding of the interaction of sea water phosphate with carbonate minerals. An uptake of phosphate by ikaite within sea ice, for instance, could contribute to phosphate enrichment relative to surface oceanic water (Hu et al. 2014; Jones et al. 2023) and, therefore, might be an important abiotic process in the nutrient dynamics of Antarctic landfast sea ice. For ikaite, however, such an incorporation of phosphate is not evident yet. Although a significant depletion of aqueous phosphate was observed during the onset of ikaite precipitation by Hu et al. (2014), ikaite samples from sea-ice growth experiments and natural surface ice did not reveal a significant uptake

of phosphate (Hu and Wang 2020). In this context, a recent study by Jones et al. (2023) showed that aqueous phosphate concentrations were inversely correlated with the formation of ikaite in sea ice.

Besides phosphate coprecipitation, the fundamental growth kinetics of ikaite is not completely understood. The formation of hydrated ikaite, in contrast to anhydrous calcium carbonate minerals such as calcite, does not involve extensive dehydration of aqueous complexes, but most likely requires an ordered assembling of the hydrated $CaCO_3^0$ ion pairs within the aqueous solution (Buchardt et al. 2001; Chaka 2018; Stockmann et al. 2018; Strohm et al. 2022). This discrepancy impedes a derivation of ikaite growth kinetics from anhydrous calcium carbonate minerals. Ikaite growth kinetics as well as phosphate uptake, however, might have important implications for the role of ikaite as an abiotic factor for seasonal fluctuations in dissolved inorganic carbon, alkalinity, and phosphate in sea ice. This study, therefore, aims at contributing to an improvement of the knowledge of ikaite growth kinetics and phosphate incorporation by conducting seeded growth experiments of ikaite in phosphate-containing solutions.

2 Materials and Methods

Aqueous solutions for seed syntheses and growth experiments were prepared by dissolving reagent grade $CaCl_2 \times 2H_2O$, NaCl, NaOH, $NaHCO_3$, NaH_2PO_4, K_2CO_3, KOH and K_2HPO_4 in deionized water (resistivity 18.2 MΩ cm). Ikaite seed crystals for growth experiments were synthesized following the procedure of Bischoff et al. (1993b) by mixing 100 ml each of 0.1 M $CaCl_2$ and K_2CO_3 solutions into a 0.04 M KOH solution (400 ml) at 1 °C. $CaCl_2$ and K_2CO_3 solutions were added dropwise through two separate channels of a peristaltic pump (*Ismatec* IPC-N) with a flow rate of 0.8—1 ml/min. Simultaneously, a K_2HPO_4 solution was added to the mixture yielding phosphate concentrations of 33–200 μM throughout the synthesis. Upon mixing, the solutions were kept at 1 °C under stirring for 24 h before the precipitate was filtered, washed with ethanol ($T = -18$ °C) and stored at -18 °C to ensure the persistence of ikaite seeds. Furthermore, calcite seeds for growth experiments were synthesized by temperature-induced transformation of ikaite in order to yield a synthetically disintegrated ikaite as a proxy for the manifold types of decomposed ikaite specimens (e.g. Boch et al. 2015; Bischoff et al. 1993a; Németh et al. 2022; Schultz et al. 2023; Vickers et al. 2022). For this, ikaite seeds were first synthesized as described above and subsequently exposed to temperature fluctuations (temperature maximum 10 °C for 24 h) to induce transformation into calcite.

Growth experiments were carried out using 1.5 g of seed crystals in a PFA cryo-mixed-flow reactor (CMFR, total reactor volume: 120 ml) similar to the experiments described in detail by Lindner and Jordan (2018) and Saldi et al. (2021). To maintain a constant temperature of 1 °C, experiments were conducted in a cooling incubator. The total experimental run time ranged from 22 to 46 h. Inlet solutions were cooled by the cooling incubator and injected into the reactor from two separate PE containers using two channels of a peristaltic pump. Within the reactor, the solutions were mixed with a Teflon-coated stirring bar. In order to prevent a loss of crystals from the reactor, the effluent solution was filtered through a PTFE membrane filter with a pore size of 0.45 μm. The effluent solution was sampled at time intervals of several hours. Each solution volume was divided into two. One subsample was utilized for pH and alkalinity measurements; the other was acidified with ultrapure concentrated HNO_3 and used for Ca and P analyses. pH was measured

immediately after sampling at 25 °C using a standard glass electrode calibrated with NIST certified pH 4.01, 7.01 and 10.01 buffer solutions. Total alkalinity was determined by potentiometric end-point titrations with and uncertainty of $\pm 2\%$ (detection limit: 5×10^{-5} eq/l) using a *Schott* TA 10plus automatic titrator and 0.01 M or 0.05 M HCl standard solution. Ca concentrations were determined by flame atomic absorption spectroscopy (AAS) using a *PerkinElmer* AANalyst 400 atomic absorption spectrometer with an uncertainty of $\pm 2\%$ and a detection limit of 1×10^{-6} M. P concentrations were measured by inductively coupled plasma optical emission spectroscopy (ICP-OES) (*Horiba* Ultima 2) with an uncertainty of $\pm 1.5\%$ and a detection limit of 1×10^{-6} M. Aqueous speciations and saturations of solutions relative to the solid phases of interest were modelled with the geochemical code PHREEQC version 3.7.0 (Parkhurst and Appelo 2013) using the llnl database. Solubility constants of ikaite (log $K_{sp} = 0.15981 - 2011.1/T$, Bischoff et al. 1993b), vaterite (log $K_{sp} = -172.1295 - 0.077993\ T + 3074.688/T + 71.595\ \log T$, Plummer and Busenberg 1982), amorphous calcium carbonate (ACC, log $K_{sp} = -12.919 + 0.054538\ T - 0.0001096\ T^2$, Brečević and Nielsen 1989), and the carbonic acid dissociation constants from Millero et al. (2007) were inserted in the llnl database. The saturation state Ω was defined as $\Omega = \frac{IAP}{K_{sp}}$ where *IAP* stands for the ionic activity product and K_{sp} for the solubility product of the mineral phase.

Compositions of the inlet solutions of CMFR growth experiments are listed in Table 1. Ionic strength of inlet solutions was adjusted to 0.1 M with NaCl, while small amounts of 1 M NaOH solution were added to set the pH to ~8.5. Each run was conducted at constant flow rate. Once constant outlet fluid composition had been reached, steady-state condition was approximated. For each steady-state condition, the growth rate (R) of ikaite was calculated by

$$R = \frac{\Delta \text{Ca}\, F}{m\, A_S} \tag{1}$$

where ΔCa is the difference of the Ca concentration between inlet and outlet solution, F is the outlet flow rate, m is the mass of the crystals, and A_S is the specific surface area. To approximate the specific surface area of ikaite seed crystals, an average crystal diameter of 50 μm was estimated from cryo-SEM images. This diameter was implemented in a cubic shape model, giving a specific surface area of 894 cm^2/g for the ikaite seed crystals.

Crystal powders were analysed before and after growth experiments by X-ray powder diffraction (XRD, *Bruker* D8 Advance A25, CuKα$_1$ radiation $\lambda = 1.5406$ Å) with scattering angles of $10° \leq 2\theta \leq 60°$ and a short measurement time of 12 min to prevent a temperature-induced phase transition during analyses. Cryoscanning electron microscopy (cryo-SEM; Quanta 250 FEG FEI, equipped with a cool stage) was used to visualize crystal powders. Images were taken using an accelerating voltage of 15 kV and a gaseous secondary electron detector (GSED).

3 Results

3.1 Analysis of Solids

Cryo-SEM images of the synthesized ikaite seeds before growth experiments revealed a homogeneous euhedral morphology (Fig. 1a). In contrast, the seeds, which have undergone an additional subsequent temperature-induced transformation into calcite, comprise

Table 1 Compositions of cryo-mixed-flow reactor inlet solutions and effluent solutions at steady-state conditions for the growth experiments conducted in this study

Sample	Seed crystals	Flowrate (ml/min)	pH (25 °C)	Total alkalinity (meq/l)	Ca (mM)	P (mM)	Δ total alkalinity (meq/l)	ΔCa (mM)	ΔP (mM)	estimated A_S (cm²)	Ω_{ikaite}
Ika_1_inlet			8.64	50.58	1.518	0.190					3.8
Ika_1_1	ikaite	0.71	8.45	49.73	0.819	0.189	− 0.85	− 0.698	− 0.001	984	1.4
Ika_1_2	"	0.71	8.48	49.68	0.817	0.195	− 0.90	− 0.701	0.005	984	1.5
Ika_1_3	"	0.71	8.47	49.63	0.823	0.199	− 0.95	− 0.695	0.009	984	1.5
Ika_2_inlet			8.49	49.76	1.303	n.d.					2.5
Ika_2_1	ikaite	0.61	8.53	n.d.^a	0.656	n.d.	n.d.	− 0.647	n.d.	984	1.3
Ika_2_2	"	0.61	8.54	48.98	0.653	n.d.	− 0.78	− 0.651	n.d.	984	1.3
Ika_2_3	"	0.61	8.54	49.09	0.643	n.d.	− 0.67	− 0.661	n.d.	984	1.3
Ika_3_inlet			8.41	46.91	4.189	n.d.					6.9
Ika_3_1	ikaite	0.82	8.25	46.27	2.252	n.d.	− 0.64	− 1.937	n.d.	984	2.6
Ika_3_2	"	0.82	8.26	46.31	2.224	n.d.	− 0.60	− 1.965	n.d.	984	2.6
Ika_4_inlet			8.25	61.71	7.329	n.d.					11
Ika_4_1	ikaite	0.77	8.28	n.d.^a	3.456	n.d.	n.d.	− 3.947	n.d.	984	4.8
Ika_4_2	"	0.76	8.29	55.02	3.376	n.d.	− 6.69	− 3.953	n.d.	984	4.9
Ika_8_inlet			8.75	50.25	2.710	0.186					8.1
Ika_8_1	calcite	0.60	8.42	46.23	1.040	0.188	− 4.02	− 1.670	0.002	n.d.	1.7
Ika_8_2	"	0.60	8.44	46.38	1.020	0.190	− 3.87	− 1.690	0.004	n.d.	1.7
Ika_13_inlet			8.45	15.19	3.874	0.193					2.7
Ika_13_1	calcite	0.58	8.34	14.18	3.366	0.202	− 1.01	− 0.508	0.009	n.d.	1.7
Ika_13_2	"	0.58	8.35	14.10	3.335	0.198	− 1.09	− 0.539	0.005	n.d.	1.7
Ika_15_inlet			8.60	24.50	4.954	0.191					7.1
Ika_15_1	calcite	0.58	8.30	n.d.^a	3.715	n.d.	n.d.	− 1.239	n.d.	n.d.	2.8
Ika_15_2	"	0.58	8.34	22.40	3.666	0.197	− 2.10	− 1.289	0.006	n.d.	2.9

[a] n.d. = not determined. When alkalinity was not determined, it was approximated for the calculation of Ω_{ikaite} by stoichiometrically decreasing the initial alkalinity of the solution by twice the corresponding Ca^{2+} decrease
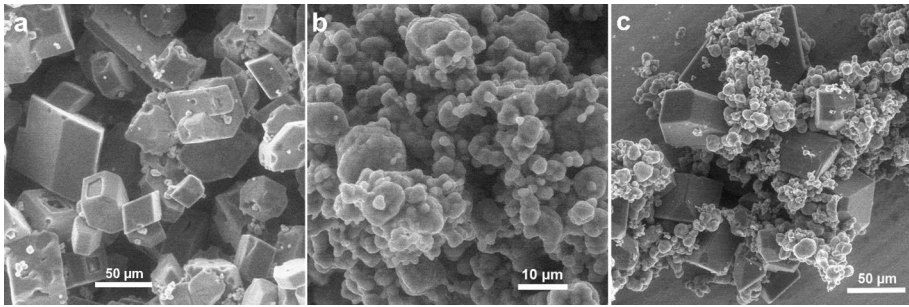
Fig. 1 Cryo-SEM images of synthesized seeds and crystals retrieved from CMFR experiment. **a** Euhedral ikaite seed crystals before growth experiment. **b** Anhedral calcite seed crystals before growth experiment. **c** Newly formed euhedral ikaite crystals coexisting with anhedral crystals after growth experiment (Ika_15)

spherical and partially coalescing anhedral aggregates (Fig. 1b). After the growth experiments, these calcite aggregates remained unaltered and coexisted with euhedral ikaite crystals, which newly formed during the experiment (Fig. 1c). X-ray powder diffraction analyses of the powders retrieved from these growth experiments confirm the coexistence of calcite with a significant amount of ikaite (Fig. 2). For ikaite-seeded experiments, X-ray diffractograms of crystals retrieved from CMFR reactor revealed ikaite (Fig. 3). The minor traces of calcite which were detected by X-ray phase analysis of ikaite seeds ($2\theta \approx 29.45$) had no impact on the growth rates in ikaite-seeded experiments (Ika_1–Ika_4) as they mostly reflect the artefactual transformation of ikaite in air during the time of X-ray analysis rather than the calcite formation during the experiments. Although all reactor solutions were supersaturated vs. hydroxyapatite, no sign of this phase was found by XRD.
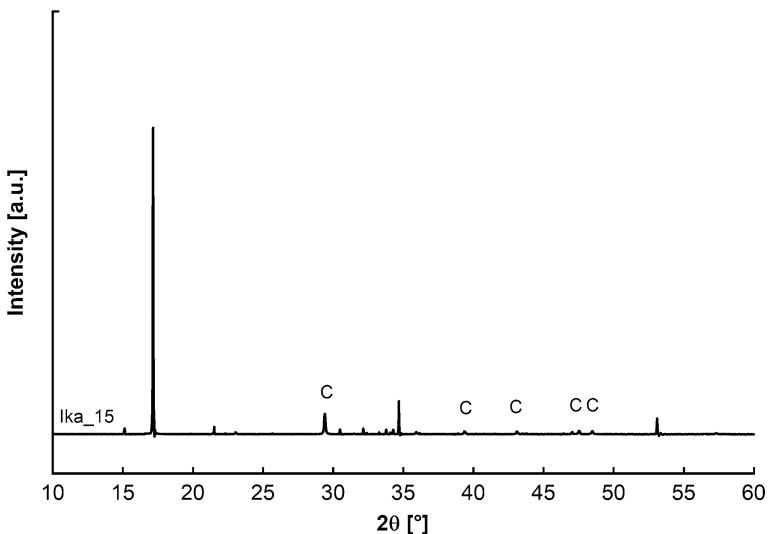
Fig. 2 X-ray powder diffraction pattern ($CuK\alpha_1$) of crystals retrieved from calcite-seeded growth experiment Ika_15. Diffraction peaks correspond to calcite (C) and newly formed ikaite
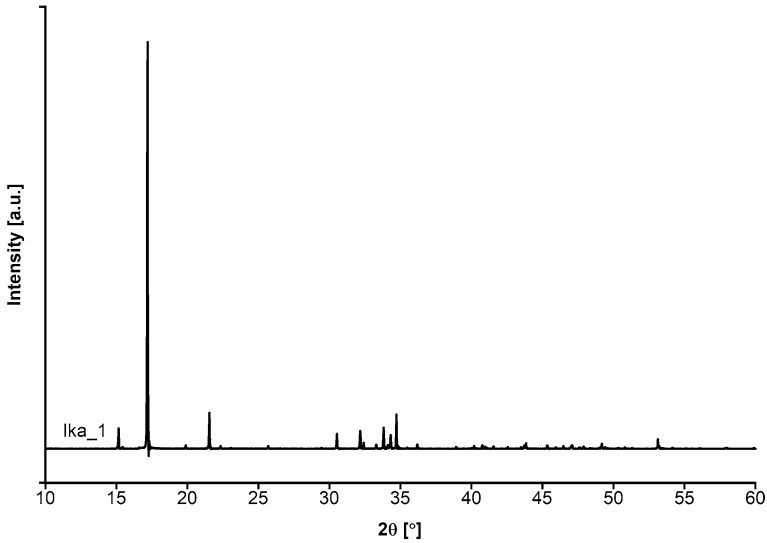
Fig. 3 X-ray powder diffraction pattern (CuKα₁) of crystals retrieved from ikaite-seeded growth experiment Ika_1. Diffraction peaks correspond to ikaite

3.2 Chemical Analysis of Solutions

Analyses of the inlet and outlet solutions of cryo-MFR experiments were performed for each run and are summarized in Table 1, which reports the compositions of the effluent solutions of the reactor at steady-state conditions. In all runs, the samples of the effluent revealed decreased Ca concentrations and total alkalinity relative to the corresponding inlet solutions (ΔCa and Δ tot. alk) indicating substantial growth within the reactor. P concentrations, in contrast, remained constant in all tested growth experiments.

3.3 Growth Kinetics of Ikaite

Although ikaite growth was evident from XRD and solution analyses for both ikaite- and calcite-seeded experiments, surface normalized growth rates could only be derived from ikaite-seeded experiments (Ika_1–Ika_4). In calcite-seeded experiments (Ika_8, Ika_13, Ika_15), the unknown length of the ikaite nucleation period negated any surface area normalization of the detected consumption of material by the growing ikaite within the reactor. This applies all the more as some volume nucleation was observed additionally to surface nucleation at the reactor walls and calcite seeds.

Ikaite-seeded experiments (Ika_1–Ika_4) provided surface normalized growth rates unequivocally, although trace amounts of freshly formed ikaite crystals were also observed in the experiments. Both growth of initial ikaite seed crystals and nucleation and growth of new ikaite crystals led to an increase of the ikaite surface area within the reactor during the experimental runs. While the increase in surface area resulting from nucleation of new ikaite crystals was negligible, the increase in surface area resulting from the growth of ikaite seeds was apparent and, therefore, considered in the rate calculations. The increase

in ikaite surface area was calculated from the measured ΔCa values and the corresponding ikaite mass increase, assuming that the specific surface area (A_S) of the solid remained constant. Mean growth rates at steady-state conditions (Ika_1–Ika_4) were plotted as a function of the fluid saturation ratio with respect to ikaite (Ω_{ikaite}) (Fig. 4).

To calculate the rate constant k and the reaction order n of ikaite growth, the empirical equation

$$R = k(\Omega - 1)^n, \tag{2}$$

which has been commonly used for the growth of calcium carbonate minerals (e.g. Busenberg and Plummer 1986; Dromgoole and Walter 1990; Gutjahr et al. 1996; Morse et al. 2007; Nancollas and Reddy 1971), was used to generate a fit of the measured growth rates (Fig. 5). The best fit of the experimental data yielded a reaction order $n = 0.8 \pm 0.3$ and a rate constant $k = 0.10 \pm 0.03$ µmol/m^2/s.

4 Discussion

4.1 Growth of Ikaite

In calcite-seeded growth experiments (Ika_8, Ika_13 and Ika_15), newly formed ikaite led to a decrease of Ca concentrations and total alkalinity relative to inlet solutions. As indicated by cryo-SEM images (Fig. 1), calcite seeds did not reveal any significant growth during CMFR experiments. Because the calcite seeds were synthesized from ikaite via a temperature-induced transformation, no other chemical component than the phosphate added to the CMFR inlet solution is the likely cause of the observed absence of noticeable calcite growth.

The reduction of calcite growth to an imperceptible amount is an explicit indicator for the phosphate solution concentration being high enough to potentially influence ikaite
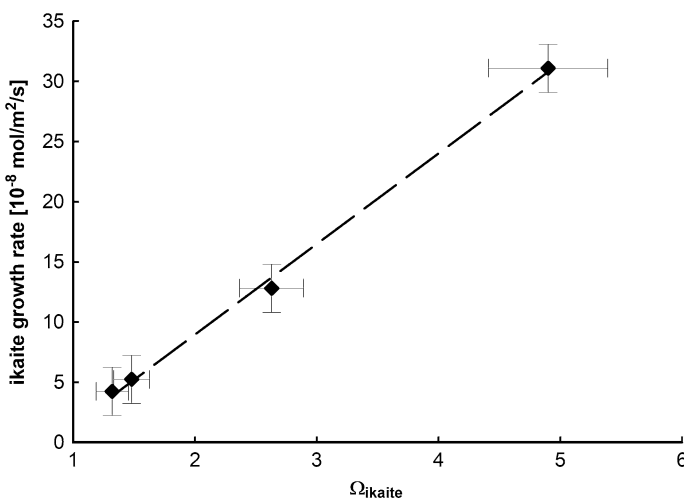

Fig. 4 CMFR growth rates of ikaite as a function of saturation ratio. The dashed line represents the linear regression of the growth rates
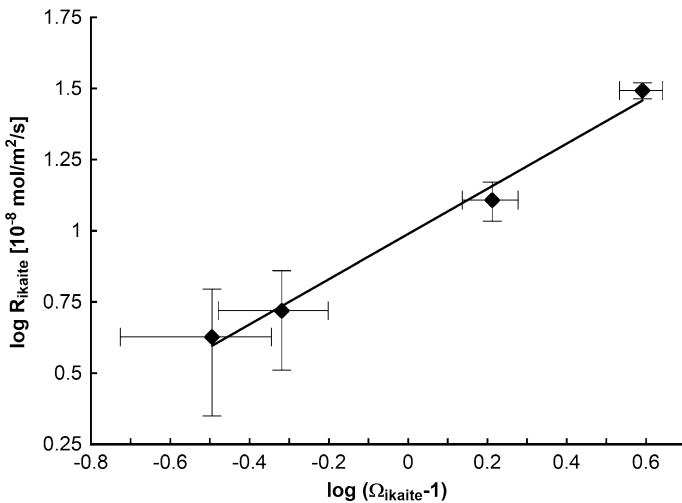
Fig. 5 Logarithmic plot of ikaite growth rates as a function of degree of supersaturation with respect to ikaite. The linear regression drawn on the plot provides a reaction order $n = 0.8 \pm 0.3$ and a rate constant $k = 0.10 \pm 0.03$ μmol/m²/s for Eq. (2)

growth as well. Ikaite growth, however, was not noticeably influenced by the added phosphate, which supports the results of Bischoff et al. 1993b, who revealed no detectable inhibition of ikaite crystallization by phosphate, while the precipitation of calcite, aragonite and vaterite was suppressed. Although the growing ikaite crystals led to a detectable Ca withdrawal in our calcite-seeded experiments, the impossibility of normalizing this withdrawal to the temporal development of the ikaite surface area disabled the calculation of ikaite growth rates. Thus, surface area normalized growth rates could be derived from ikaite-seeded experiments exclusively (Ika_1–Ika_4).

A plot of ikaite growth rates as a function of the corresponding saturation sate of the aqueous solutions with respect to this phase (Ω_{ikaite}) revealed a linear dependence of rates on supersaturation (Fig. 4). Our growth rate constant ($k = 0.10 \pm 0.03$ μmol/m²/s) is higher than the rate constant of approx. 0.03 μmol/m²/s determined by Papadimitriou et al. (2014) which was derived from precipitation in seawater and seawater-derived brines at salinities $S = 66$ ‰ ($T = -3.6$ °C) and $S = 102$ ‰ ($T = -5.9$ °C). The increased value in our study relative to the one published by Papadimitriou et al. (2014) might be explained by different solution conditions. Although Papadimitriou et al. (2014) did not detect a significant difference of rate constants within their salinity and temperature interval, our rate constant obtained from solutions with tremendously lower salinity and slightly higher temperature (ionic strength of 0.1 M corresponding to $S \approx 6$‰, $T = +1.0$ °C) might point towards either a weak direct correlation of the rate constant with temperature or an inverse correlation of the constant with salinity or both. Whether the aqueous phosphate in our experiments compared those of Papadimitriou et al. (2014) influences ikaite growth cannot be assessed as the phosphate concentrations of the poorly defined solutions used by Papadimitriou et al. (2014) are unknown.

The reaction order of $n = 0.8 \pm 0.3$, which was derived from the empirical equation $R = k(\Omega - 1)^n$, points towards first-order reaction kinetics. This is in good agreement with the reaction order of $n = 1.23 \pm 0.42$ obtained by Papadimitriou et al. (2014) and in contrast to growth kinetics of calcite in sea water at 25 °C. For the latter, the empirical rate equation

frequently indicated second to third-order reaction kinetics (e.g. Burton and Walter 1990; Lopez et al. 2009; Mucci 1986; Zhong and Mucci 1993). Furthermore, the presence of phosphate in artificial sea water led to a slight increase of the reaction order of calcite relative to that determined for phosphate-free solution (Mucci 1986). Such an increase of the reaction order can be ruled out for ikaite as phosphate does not retard ikaite growth in similar way to calcite growth (Bischoff et al. 1993b; Hu et al. 2015). For ikaite, the obtained first-order reaction kinetics for growth in phosphate-containing solutions implies a transport or adsorption process as the rate controlling mechanism (e.g. Nielsen 1983). Although this macroscopic approach does not provide direct evidence for the growth rate controlling reactions, as microscopic surface processes may lead to deviations from the predictions of rate laws (Teng et al. 2000), a transport or adsorption-controlled growth mechanism is consistent with the way an extremely hydrated phase such as ikaite could grow. The classical model of calcite growth via attachment, dehydration and incorporation of growth units (e.g. Gratz et al. 1993; Morse et al. 2007) may not apply to ikaite as a complete dehydration of attaching species is not required. Ikaite growth might simply comprise an incorporation of a $CaCO_3^0$ ion pair together with six water molecules. Density functional theory (DFT) calculations of Chaka (2018) confirmed this low energy pathway of crystallization via the assemblage of aqueous $CaCO_3^0 \times 6H_2O$ ion pair complexes. This low energy pathway was further corroborated by low interfacial energies of ikaite nuclei (Strohm et al. 2022).

4.2 The Insignificance of Phosphate Uptake by Ikaite During Growth

In the CMFR growth experiments (saturation state $1.5 \leq \Omega_{ikaite} \leq 2.9$), measured phosphate concentrations revealed no evidence of phosphate incorporation into ikaite crystals. During ikaite seed synthesis, which was conducted at much higher supersaturation, a phosphate uptake cannot be ruled out per se as phosphate partitioning between precipitate and solution might be increasing at an increasing distance from equilibrium. Furthermore, a significant withdrawal of aqueous phosphate concomitant to the onset of ikaite precipitation was observed in a laboratory study by Hu et al. (2014). However, any significant phosphate uptake of ikaite during our seed synthesis is questionable. Disintegration of ikaite causes the release of its weakly bonded water (e.g. Németh et al. 2022; Vickers et al. 2022). If phosphate had been taken up during ikaite seed synthesis, the subsequent transformation of the filtered ikaite seeds into calcite would have been taken place in a phosphate-containing solution. Within such a phosphate-containing solution, however, the formation of calcite is impeded, as even minor amounts of phosphate (1 μM) are known to interfere with the nucleation of calcite (Lin and Singer 2006). This inhibition of calcite nucleation and promotion of ikaite appearance (or persistence) was found to apply at temperatures up to 25 °C (Clarkson et al. 1992). As the transformation of our filtered ikaite seeds into calcite took place without any problems, it can be assumed that the phosphate uptake from solution during seed synthesis due to coprecipitation with ikaite is likely very limited. Furthermore, it is noteworthy that the $[Ca^{2+}]:[CO_3^{2-}]$ ratio varied in our growth experiments (Ika_1: $[Ca^{2+}]:[CO_3^{2-}] \approx 0.6$, Ika_13: $[Ca^{2+}]:[CO_3^{2-}] \approx 12$). Thus, the results also show that a decreased $[CO_3^{2-}]$ concentration does not promote substitution of carbonate by phosphate ions during ikaite growth. Substitution of these anions might be expected if carbonate and phosphate ions were competing for incorporation.

The lack of phosphate coprecipitation with ikaite contrasts with calcite. While laboratory studies showed that calcite was capable of incorporating detectable amounts of phosphate from solution during growth (Hartley et al. 1997; House and Donaldson

1986; Ishikawa and Ichikuni 1981), phosphate coprecipitation is not observed during ikaite growth in our study. The distinct growth mechanisms of the different calcium carbonate phases might explain this discrepancy. The incorporation of adsorbed phosphate into calcite most likely occurs at active growth surface sites (House and Donaldson 1986), which is in agreement with the classical model of calcite growth. Incorporation of phosphate ions into growing ikaite by substitution of carbonate ions, in contrast, might be less compatible with a growth mechanism via an assembling of hydrous $CaCO_3^0$ ion pair complexes.

In summary, there was no sign of phosphate uptake by ikaite from all the experiments performed in this study. This finding supports the results of Hu and Wang (2020), who did not obtain a detectable coprecipitation of phosphate with ikaite in samples grown in sea ice. Based on the experimental data, therefore, it needs to be taken into account that phosphate coprecipitation with ikaite in sea ice may not necessarily contribute significantly to seasonal phosphate accumulations in Antarctic landfast and pack ice (e.g. Cozzi 2008; Fripiat et al. 2017; Jones et al. 2023; Meiners et al. 2011). Even though ikaite formation in sea ice may occur with high temporal dynamics (Papadimitriou et al. 2014; Rysgaard et al. 2014) and, thus, nucleation and growth conditions of ikaite in sea ice might not exactly match the conditions of this study in all respects, the absence of any signs of phosphate uptake by ikaite rather supports the importance of previously proposed biotic pathways like phosphate remineralization in biofilm microenvironments and phosphate accumulation due to sea ice algae (Fripiat et al. 2017; van der Linden et al. 2020).

5 Conclusions

The presence of phosphate in the aqueous solutions revealed no detectable impact on the growth of ikaite for the experimental conditions tested in this study. An uptake of significant amounts of phosphate can be precluded at low supersaturation conditions ($1.5 \leq \Omega_{ikaite} \leq 2.9$). Furthermore, a retardation of growth, as known from calcite growth studies, was not evident for ikaite. Measured growth rates of ikaite indicated a first-order rate law which supports a growth mechanism different from anhydrous calcium carbonate minerals involving a dominant role of the attachment of hydrous $CaCO_3^0$ complexes. This growth mechanism is suggestive of a low energy pathway, which does not require extensive dehydration of attaching species and likely does not allow for substantial substitution of carbonate by phosphate ions.

Author contributions S.B.S. performed the experiments and drafted the manuscript. All authors contributed to the research and reviewed the manuscript.

Declarations

Conflict of interest The authors declare no competing financial and non-financial interests.

References

Bischoff JL, Rosenbauer RJ, Fitzpatrick JA, Stafford TW Jr (1993a) Ikaite precipitation by mixing of shoreline springs and lake water, Mono Lake, California, USA. Geochimica Et Cosmochimica 57:3855–3865. https://doi.org/10.1016/0016-7037(93)90339-X

Bischoff JL, Fitzpatrick JA, Rosenbauer RJ (1993b) The solubility and stabilization of ikaite ($CaCO_3 \cdot 6H2O$) from 0° to 25 °C: environmental and paleoclimatic implications for Thinolite Tufa. J Geol 101:21–33. https://doi.org/10.1086/648194

Boch R, Dietzel M, Reichl P, Leis A, Baldermann A, Mittermayr F, Pölt P (2015) Rapid ikaite ($CaCO_3 \cdot 6H_2O$) crystallization in a man-made river bed: hydrogeochemical monitoring of a rarely documented mineral formation. Appl Geochem 63:366–379. https://doi.org/10.1016/j.apgeochem.2015.10.003

Brečević L, Nielsen AE (1989) Solubility of amorphous calcium carbonate. J Cryst Growth 98:504–510. https://doi.org/10.1016/0022-0248(89)90168-1

Buchardt B, Israelson C, Seaman P, Stockmann G (2001) Ikaite tufa towers in Ikka Fjord, southwest Greenland: their formation by mixing of seawater and alkaline spring water. J Sediment Res 71:176–189. https://doi.org/10.1306/042800710176

Burton EA, Walter LM (1990) The role of pH in phosphate inhibition of calcite and aragonite precipitation rates in seawater. Geochim Cosmochim Acta 54:797–808. https://doi.org/10.1016/0016-7037(90)90374-T

Busenberg E, Plummer LN (1986) A comparative study of the dissolution and crystal growth kinetics of calcite and aragonite. Stud Diagenesis 1578:139–168

Chaka AM (2018) Ab initio thermodynamics of hydrated calcium carbonates and calcium analogues of magnesium carbonates: implications for carbonate crystallization pathways. ACS Earth Space Chem 2:210–224. https://doi.org/10.1021/acsearthspacechem.7b00101

Clarkson JR, Price TJ, Adams CJ (1992) Role of metastable phases in the spontaneous precipitation of calcium carbonate. J Chem Soc Faraday Trans 88:243–249. https://doi.org/10.1039/FT9928800243

Cozzi S (2008) High-resolution trends of nutrients, DOM and nitrogen uptake in the annual sea ice at Terra Nova Bay, Ross Sea. Antarct Sci 20:441–454. https://doi.org/10.1017/S0954102008001247

Delille B, Vancoppenolle M, Geilfus N-X, Tilbrook B, Lannuzel D, Schoemann V, Becquevort S, Carnat G, Delille D, Lancelot C, Chou L, Dieckmann GS, Tison J-L (2014) Southern Ocean CO_2 sink: the contribution of the sea ice. J Geophys Res Oceans 119:6340–6355. https://doi.org/10.1002/2014JC009941

Dieckmann GS, Nehrke G, Papadimitriou S, Göttlicher J, Steininger R, Kennedy H, Wolf-Gladrow D, Thomas DN (2008) Calcium carbonate as ikaite crystals in Antarctic sea ice. Geophys Res Lett. https://doi.org/10.1029/2008GL033540

Dieckmann GS, Nehrke G, Uhlig C, Göttlicher J, Gerland S, Granskog MA, Thomas DN (2010) Brief Communication: Ikaite ($CaCO_3 \cdot 6H_2O$) discovered in Arctic sea ice. Cryosphere 4:227–230. https://doi.org/10.5194/tc-4-227-2010

Dromgoole EL, Walter LM (1990) Inhibition of calcite growth rates by Mn^{2+} in $CaCl_2$ solutions at 10, 25, and 50 C. Geochim Cosmochim Acta 54:2991–3000. https://doi.org/10.1016/0016-7037(90)90116-3

Fripiat F, Meiners KM, Vancoppenolle M, Papadimitriou S, Thomas DN, Ackley SF, Arrigo KR, Carnat G, Cozzi S, Delille B, Dieckmann GS, Dunbar RB, Fransson A, Kattner G, Kennedy H, Lannuzel D, Munro DR, Nomura D, Rintala J-M, Schoemann V, Stefels J, Steiner N, Tison J-L (2017) Macro-nutrient concentrations in Antarctic pack ice: overall patterns and overlooked processes. Elem Sci Anthropocene. https://doi.org/10.1525/elementa.217

Geilfus N-X, Carnat G, Dieckmann GS, Halden N, Nehrke G, Papakyriakou T, Tison J-L, Delille B (2013) First estimates of the contribution of $CaCO_3$ precipitation to the release of CO_2 to the atmosphere during young sea ice growth. J Geophys Res Oceans 118:244–255. https://doi.org/10.1029/2012JC007980

Geilfus N-X, Galley RJ, Else BGT, Campbell K, Papakyriakou T, Crabeck O, Lemes M, Delille B, Rysgaard S (2016) Estimates of ikaite export from sea ice to the underlying seawater in a sea ice–seawater mesocosm. Cryosphere 10:2173–2189. https://doi.org/10.5194/tc-10-2173-2016

Gratz AJ, Hillner PE, Hansma PK (1993) Step dynamics and spiral growth on calcite. Geochim Cosmochim Acta 57:491–495. https://doi.org/10.1016/0016-7037(93)90449-7

Gutjahr A, Dabringhaus H, Lacmann R (1996) Studies of the growth and dissolution kinetics of the $CaCO_3$ polymorphs calcite and aragonite I. Growth and dissolution rates in water. J Cryst Growth 158:296–309. https://doi.org/10.1016/0022-0248(95)00446-7

Habraken WJEM, Masic A, Bertinetti L, Al-Sawalmih A, Glazer L, Bentov S, Fratzl P, Sagi A, Aichmayer B, Berman A (2015) Layered growth of crayfish gastrolith: about the stability of amorphous calcium carbonate and role of additives. J Struct Biol 189:28–36. https://doi.org/10.1016/j.jsb.2014.11.003

Hartley AM, House WA, Callow ME, Leadbeater B (1997) Coprecipitation of phosphate with calcite in the presence of photosynthesizing green algae. Water Res 31:2261–2268. https://doi.org/10.1016/S0043-1354(97)00103-6

House WA, Donaldson L (1986) Adsorption and coprecipitation of phosphate on calcite. J Colloid Interface Sci 112:309–324. https://doi.org/10.1016/0021-9797(86)90101-3

Hu Y-B, Wang F (2020) Effect of ikaite precipitation on phosphate removal in sea ice. Polar Res. https://doi.org/10.33265/polar.v39.3413

Hu Y-B, Dieckmann GS, Wolf-Gladrow DA, Nehrke G (2014) Laboratory study on coprecipitation of phosphate with ikaite in sea ice. J Geophys Res Oceans 119:7007–7015. https://doi.org/10.1002/2014JC010079

Hu Y-B, Wolthers M, Wolf-Gladrow DA, Nehrke G (2015) Effect of pH and phosphate on calcium carbonate polymorphs precipitated at near-freezing temperature. Cryst Growth Des 15:1596–1601. https://doi.org/10.1021/cg500829p

Ishikawa M, Ichikuni M (1981) Coprecipitation of phosphate with calcite. Geochem J 15:283–288. https://doi.org/10.2343/geochemj.15.283

Ito T (1996) Ikaite from cold spring water at Shiowakka, Hokkaido, Japan. J Mm Petr Econ Geol 91:209–219. https://doi.org/10.2343/geochemj.32.267

Johnston J, Merwin HE, Williams ED (1916) The several forms of calcium carbonate. Am J Sci 4(246):473–512

Jones EM, Henley SF, van Leeuwe MA, Stefels J, Meredith MP, Fenton M, Venables HJ (2023) Carbon and nutrient cycling in Antarctic landfast sea ice from winter to summer. Limnol Oceanogr 68:208–231. https://doi.org/10.1002/lno.12260

Kababya S, Gal A, Kahil K, Weiner S, Addadi L, Schmidt A (2015) Phosphate-water interplay tunes amorphous calcium carbonate metastability: spontaneous phase separation and crystallization vs stabilization viewed by solid state NMR. J Am Chem Soc 137:990–998. https://doi.org/10.1021/ja511869g

Kitano Y, Minoru O, Masatoshi I (1978) Uptake of phosphate ions by calcium carbonate. Geochem J 12:29–37. https://doi.org/10.2343/geochemj.12.29

Lin Y-P, Singer PC (2006) Inhibition of calcite precipitation by orthophosphate: speciation and thermodynamic considerations. Geochim Cosmochim Acta 70:2530–2539. https://doi.org/10.1016/j.gca.2006.03.002

Lindner M, Jordan G (2018) On the growth of witherite and its replacement by the Mg-bearing double carbonate norsethite: implications for the dolomite problem. Am Miner 103:252–259. https://doi.org/10.2138/am-2018-6232

Lopez O, Zuddas P, Faivre D (2009) The influence of temperature and seawater composition on calcite crystal growth mechanisms and kinetics: implications for Mg incorporation in calcite lattice. Geochim Cosmochim Acta 73:337–347. https://doi.org/10.1016/j.gca.2008.10.022

Marland G (1975) The stability of of $CaCO_3 \cdot 6H_2O$ (ikaite). Geochim Cosmochim Acta 39:83–91. https://doi.org/10.1016/0016-7037(75)90186-6

Meiners KM, Norman L, Granskog MA, Krell A, Heil P, Thomas DN (2011) Physico-ecobiogeochemistry of East Antarctic pack ice during the winter-spring transition. Deep Sea Res Part II 58:1172–1181. https://doi.org/10.1016/j.dsr2.2010.10.033

Millero FJ (2013) Chemical oceanography, 4th edn. CRC Press, Boca Raton. https://doi.org/10.1201/b14753

Millero F, Huang F, Graham T, Pierrot D (2007) The dissociation of carbonic acid in NaCl solutions as a function of concentration and temperature. Geochim Cosmochim Acta 71:46–55. https://doi.org/10.1016/j.gca.2006.08.041

Morse JW, Arvidson RS, Lüttge A (2007) Calcium carbonate formation and dissolution. Chem Rev 107:342–381. https://doi.org/10.1021/cr050358j

Mucci A (1986) Growth kinetics and composition of magnesian calcite overgrowths precipitated from seawater: quantitative influence of orthophosphate ions. Geochim Cosmochim Acta 50:2255–2265. https://doi.org/10.1016/0016-7037(86)90080-3

Nancollas GH, Reddy MM (1971) The crystallization of calcium carbonate. II. Calcite growth mechanism. J Colloid Interface Sci 37:824–830. https://doi.org/10.1016/0021-9797(71)90363-8

Németh P, Töchterle P, Dublyansky Y, Stalder R, Molnár Z, Klébert S, Spötl C (2022) Tracing structural relicts of the ikaite-to-calcite transformation in cryogenic cave glendonite. Am Miner 107:1960–1967. https://doi.org/10.2138/am-2022-8162

Nielsen AE (1983) Precipitates: formations, coprecipitation, and aging. In: Kolthoff IM, Elving PJ (eds) Treatise on analytical chemistry. Wiley, New York, pp 269–347

Papadimitriou S, Kennedy H, Kennedy P, Thomas DN (2014) Kinetics of ikaite precipitation and dissolution in seawater-derived brines at sub-zero temperatures to 265 K. Geochim Cosmochim Acta 140:199–211. https://doi.org/10.1016/j.gca.2014.05.031

Parkhurst DL, Appelo CAJ (2013) Description of Input for PHREEQC version 3: a computer program for speciation, batch-reaction, one-dimensional transport, and inverse geochemical calculations. U.S. Geological survey, Denver, Colorado

Plummer LN, Busenberg E (1982) The solubilities of calcite, aragonite and vaterite in CO_2-H_2O solutions between 0 and 90 °C, and an evaluation of the aqueous model for the system $CaCO_3$-CO_2-H_2O. Geochim Cosmochim Acta 6:1011–1040. https://doi.org/10.1016/0016-7037(82)90056-4

Rysgaard S, Wang F, Galley RJ, Grimm R, Notz D, Lemes M, Geilfus N-X, Chaulk A, Hare AA, Crabeck O, Else BGT, Campbell K, Sørensen LL, Sievers J, Papakyriakou T (2014) Temporal dynamics of ikaite in experimental sea ice. Cryosphere 8:1469–1478. https://doi.org/10.5194/tc-8-1469-2014

Saldi GD, Causserand C, Schott J, Jordan G (2021) Dolomite dissolution mechanisms at acidic pH: New insights from high resolution pH-stat and mixed-flow reactor experiments associated to AFM and TEM observations. Chem Geol 584:120521. https://doi.org/10.1016/j.chemgeo.2021.120521

Schultz BP, Huggett J, Ullmann CV, Kassens H, Kölling M (2023) Links between ikaite morphology, recrystallised ikaite petrography and glendonite pseudomorphs determined from polar and deep-sea ikaite. Minerals 13:841. https://doi.org/10.3390/min13070841

Sø HU, Postma D, Jakobsen R, Larsen F (2011) Sorption of phosphate onto calcite; results from batch experiments and surface complexation modeling. Geochim Cosmochim Acta 75:2911–2923. https://doi.org/10.1016/j.gca.2011.02.031

Stockmann G, Tollefsen E, Skelton A, Brüchert V, Balic-Zunic T, Langhof J, Skogby H, Karlsson A (2018) Control of a calcite inhibitor (phosphate) and temperature on ikaite precipitation in Ikka Fjord, southwest Greenland. Appl Geochem 89:11–22. https://doi.org/10.1016/j.apgeochem.2017.11.005

Stockmann GJ, Seaman P, Balic-Zunic T, Peternell M, Sturkell E, Liljebladh B, Gyllencreutz R (2022) Mineral changes to the Tufa columns of Ikka Fjord. SW Greenl Miner 12:1430. https://doi.org/10.3390/min12111430

Strohm SB, Inckemann SE, Gao K, Schweikert M, Lemloh M-L, Schmahl WW, Jordan G (2022) On the nucleation of ikaite ($CaCO_3 \times 6H_2O$): a comparative study in the presence and absence of mineral surfaces. Chem Geol 611:121089. https://doi.org/10.1016/j.chemgeo.2022.121089

Stumm W, Leckie JO (1970) Phosphate exchange with sediments; its role in the productivity of surface waters. In: Proceedings of the 5th international water pollution research congress, San Francisco, Section:III-26/1–III/26/16

Suzuki T, Shigehiro I, Kiyoshi S (1986) Adsorption of phosphate on calcite. J Chem Soc 82:1733–1743. https://doi.org/10.1039/F19868201733

Tadier S, Rokidi S, Rey C, Combes C, Koutsoukos PG (2017) Crystal growth of aragonite in the presence of phosphate. J Cryst Growth 458:44–52. https://doi.org/10.1016/j.jcrysgro.2016.10.046

Teng HH, Dove PM, De Yoreo JJ (2000) Kinetics of calcite growth: surface processes and relationships to macroscopic rate laws. Geochim Cosmochim Acta 64:2255–2266. https://doi.org/10.1016/S0016-7037(00)00341-0

Tollefsen E, Stockmann G, Skelton A, Mörth C-M, Dupraz C, Sturkell E (2018) Chemical controls on ikaite formation. Mineral Mag 82:1119–1129. https://doi.org/10.1180/mgm.2018.110

Tollefsen E, Balic-Zunic T, Mörth C-M, Brüchert V, Lee CC, Skelton A (2020) Ikaite nucleation at 35 °C challenges the use of glendonite as a paleotemperature indicator. Sci Rep 10:1–10. https://doi.org/10.1038/s41598-020-64751-5

van der Linden FC, Tison J-L, Champenois W, Moreau S, Carnat G, Kotovitch M, Fripiat F, Deman F, Roukaerts A, Dehairs F, Wauthy S, Lourenço A, Vivier F, Haskell T, Delille B (2020) Sea ice CO_2 dynamics across seasons: impact of processes at the interfaces. J Geophys Res Oceans. https://doi.org/10.1029/2019JC015807

van der Weijden RD, Meima J, Comans RNJ (1997) Sorption and sorption reversibility of cadmium on calcite in the presence of phosphate and sulfate. Mar Chem 57:119–132. https://doi.org/10.1016/S0304-4203(97)00018-2

Vickers ML, Vickers M, Rickaby RE, Wu H, Bernasconi SM, Ullmann CV, Bohrmann G, Spielhagen RF, Kassens H, Pagh Schultz B, Alwmark C, Thibault N, Korte C (2022) The ikaite to calcite transformation: implications for palaeoclimate studies. Geochim Cosmochim Acta 334:201–216. https://doi.org/10.1016/j.gca.2022.08.001

Zhong S, Mucci A (1993) Calcite precipitation in seawater using a constant addition technique: a new overall reaction kinetic expression. Geochim Cosmochim Acta 57:1409–1417. https://doi.org/10.1016/0016-7037(93)90002-E

Zhou X, Lu Z, Rickaby REM, Domack EW, Wellner JS, Kennedy HA (2015) Ikaite abundance controlled by porewater phosphorus level: potential links to dust and productivity. J Geol 123:269–328. https://doi.org/10.1086/681918

Zou Z, Yang X, Albéric M, Heil T, Wang Q, Pokroy B, Politi Y, Bertinetti L (2020) Additives control the stability of amorphous calcium carbonate via two different mechanisms: surface adsorption versus bulk incorporation. Adv Funct Mater 30:2000003. https://doi.org/10.1002/adfm.202000003

Zou Z, Xie J, Macías-Sánchez E, Fu Z (2021) Nonclassical crystallization of amorphous calcium carbonate in the presence of phosphate ions. Cryst Growth Des 21:414–423. https://doi.org/10.1021/acs.cgd.0c01245